encit 2020

ABCM Associação Brasileira de Engenharia e Ciências Mecânicas

18th Brazilian Congress of Thermal Sciences and Engineering
November 16-20, 2020 (Online)

ENC-2020-0708
THERMODYNAMIC ANALYSIS OF AN ORC DRIVEN BY A PARABOLIC TROUGH COLLECTOR WITH NANOFLUIDS

Diogo do Carmo Zidan
Cristiana Brasil Maia
Pontifícia Universidade Católica de Minas Gerais – Av. Dom José Gaspar, 500, Coração Eucarístico, Belo Horizonte, MG
diogo.zidan@sga.pucminas.br
cristiana@pucminas.br

Abstract. *The continuous rise of world energy consumption together with the damage caused by the intense usage of fossil fuels brings a special attention in renewable energy sources. The solar energy is highlighted as a clean and abundant solution. This work studies a method to upgrade the energy generation through solar systems by applying nanofluids in a Parabolic Trough Collector (PTC) used as heat source of an Organic Rankine Cycle (ORC). Syltherm 800 is used as base fluid and to compose the nanofluid, different nanoparticle materials, such as Al_2O_3 and TiO_2, are evaluated. Toluene and Cyclohexane are also investigated as ORC operation fluids. The results expose a significant enhancement in the ORC thermal efficiency for the nanofluid with TiO_2 but a small improvement for the nanofluid with Al_2O_3. In addition, calculations demonstrated a considerable increase in the heat transfer coefficient and a significant drop in Reynolds number as the nanoparticle concentration in the nanofluid increases.*

Keywords: *Parabolic Trough Collector, Organic Rankine Cycle, Nanofluids*

1. INTRODUCTION

One of the greatest challenges faced by the world today is the continuous increase of energy consumption. A recent report from UN estimates the total world population in 7.8 billion people and the expectation is to reach 10 billion people by the end of 2057 (United Nations, 2019). According to the EIA report, it is projected that the electricity generation rises up to 79% until 2050, and even with a major evolution in renewable energy consumption, this study expects that the world will still consume more than 240 quadrillion Btu of global liquid fuels in 2050 (U.S. Energy Information Administration, 2019).

By means of that, the scientific community is encouraged to develop researches about clean energy sources and how this technology can be improved. Owusu and Asumadu-Sarkodie (2016) defined six main renewable energy sources: hydropower, biomass, geothermal, solar, wind and tidal (Owusu & Asumadu-Sarkodie, 2016). Among them, solar energy is considered one of the most abundant permanent renewable energy source, which can be used for countless applications, especially in countries with a high solar potential (Gorji & Ranjbar, 2017; Lewis & Nocera, 2007).

The energy provided from the sun is mainly harnessed by two types of technology: photovoltaic modules and solar thermal collectors (Olia et al., 2019). The photovoltaic (PV) modules directly convert the sunlight into electricity, however the PV cells efficiency are normally around 10-20% and as much as the radiation heats up the cells, the efficiency decreases (Dupeyrat et al., 2014). The solar thermal collectors take advantage of the solar energy by concentrating and absorbing the sunlight, converting into heat and transferring this energy to a working fluid which can be a liquid or a gas, for example: water, oil, molten salt, helium or air nitrogen (Kalogirou et al., 2016).

Solar thermal collectors are used for numerous applications such as water heating systems, space heating and cooling, solar refrigeration, industrial process heat, solar desalination systems, chemistry applications and solar thermal power plants (Kalogirou, 2004). Solar flat plate collectors are highly used for domestic applications and the efficiency of these systems reaches up to 70% (Jaisankar et al., 2011), but currently a large number of solar collectors are being applied on concentrating solar power (CSP) systems, which use lenses or mirrors and tracking systems to focus the sunlight into a small beam, and then used as a heat source for a conventional power plant (Nagarajan et al., 2014). Unfortunately, it is still difficult for the solar driven systems to contest the conventional and non-clean approaches. Because of that, a large number of research has been done directed on methods to improve the solar thermal collector performance and make them the best candidate for thermal processes (Delfani et al., 2016; Zamzamian et al., 2014).

A promising way to develop the solar thermal collector efficiency is to enhance the heat transfer coefficient and thermal conductivity characteristics of its working fluid, therefore it is indicated the utilization of nanofluids (Zhang et al., 2016). They consists in solid nanparticles, with a dimension usually less than 100 nm, dispersed in a base fluid. The term was first mentioned by Choi and Eastman at their study made in Argonne national laboratory, USA (Choi & Eastman,

1995). The benefits presented in the paper encouraged the scientific researches to perform new investigations over the last decade. Generally, the nanofluids can have a significantly better heat transfer aspect than conventional fluids depending on the nanoparticles material, size, shape and concentration (Maheshwary et al., 2017; Xu et al., 2019). The nanoparticles are categorized as metallic, such as Fe, Cu, Zn, Al, Au, and non-metallic such as SiO_2, TiO_2, Fe_2O_3, ZnO, CeO_2, multiwall carbon nanotubes (MWCNT), carbon nanotubes (CNT) (Bellos & Tzivanidis, 2019).

A small but increasing number of studies have been done based on the influence that the nanofluids bring to solar collectors performance (Bellos & Tzivanidis, 2017). Mwesigye et al. analyzed the efficiency of a Parabolic Trough Collector using nanofluid with Syltherm 800 as base fluid and Al_2O_3 as nanoparticles for concentrations up to 8%. The results showed a thermal efficiency enhancement of 7.6% (Mwesigye et al., 2015). The use of nanofluid in a solar driven cooling system was investigated by Abu-Hamdeh and Almitani. Improvements on convective heat transfer coefficient of 7.20-14.40%, 6.20-12.30% and 5.50-9.01% were obtained for 0.01-0.04 volume concentrations of Al_2O_3, Fe_3O_4 and ZnO nanoparticles, respectively (Abu-Hamdeh & Almitani, 2016).

There are many types of solar collector that can be used in solar power pants. Among the existing ones like solar towers, Fresnel collectors and solar dish collectors, the Parabolic Trough Collectors (PTCs) are highlighted as the most mature technology for this operation and they are used in 90% of CSP installations worldwide (Binotti et al., 2013; Grena, 2010). In order to generate clean energy, the PTC technology is highly applied as the heat source of Rankine cycles (Tzivanidis et al., 2016). In the Mojave Desert, located in California, USA, there are several solar power plants and one of them is the Abengoa facility, which uses PTC technology and has a capacity of around 280 MW, prevents the emission of about 223,440 tons of CO_2 annually (Abengoa, 2014).

In this work, an Organic Rankine Cycle (ORC) is examined with PTC as the heat source. The application of nanofluids as working fluid of the PTC is investigated, and a parametric analysis is executed seeking to study the influence of nanoparticles concentration on the PTC heat generation and consequently, the ORC thermal efficiency.

2. METHODOLOGY

This work presents a mathematical model for the nanofluid, the solar collector field and the ORC. The software EES (Engineering Equation Solver) is selected to solve the models equations. They describe the solar energy absorption by the PTC, the heat transferred to the nanofluid, which feeds the ORC boiler, and the cycle performance. Since the nanoparticles concentration, together with its material, play a big role in the nanofluid heat transfer rate, and therefore the PTC thermal efficiency, this work investigates different combinations of nanofluids and nanoparticles concentrations.

2.1 Nanofluids model

The nanofluid is the working fluid, which absorbs the heat provided from the sun irradiation, flows to the ORC boiler, transporting this heat, and returns to the PTC, completing the cycle. The base fluid selected for this work is the Syltherm 800, due to its low fouling potential, low freezing point, high temperature stability, long life and noncorrosive characteristics (Dow Corning Corporation, 1997). Syltherm 800 is a usual thermal oil with an operating temperature range between -40 and 400ºC. The nanoparticles material chosen to compose the nanofluid are Alumina (Al_2O_3) and Titanium oxide (TiO_2). The Syltherm 800 thermal properties have been taken by the EES libraries and the nanoparticles thermal properties as listed in Tab. 1.

Table 1. Nanoparticles thermal properties (Turkyilmazoglu, 2017)

Nanoparticle material	ρ (kg/m³)	Cp (J/kgK)	k (W/mK)
Alumina (Al_2O_3)	3970	765	40
Titanium oxide (TiO_2)	4250	686.2	8.9538

Since the nanofluids are a mix of a base fluid and dispersed nanoparticles, its thermal properties are calculate by correlations which merges both materials properties.

Equation (1) presents the density (ρ_{nf}) correlation (Ayatollahi et al., 2012), the specific heat (Cp_{nf}) is described by Eq. (2) (Khanafer & Vafai, 2011), the calculation of the thermal conductivity (k_{nf}) has been done by Eq. (3) (Yu & Choi, 2003) and the dynamic viscosity (μ_{nf}) is determined according to the Brinkman model, presented in Eq. (4) (Mahian et al., 2014).

$$\rho_{nf} = \rho_{bf} \cdot (1-\phi) + \rho_{np} \cdot \phi \tag{1}$$

$$Cp_{nf} = \frac{\rho_{bf} \cdot (1-\phi)}{\rho_{nf}} \cdot Cp_{bf} + \frac{\rho_{np} \cdot \phi}{\rho_{nf}} \cdot Cp_{np} \tag{2}$$

$$k_{nf} = k_{bf} \cdot \frac{k_{np} + 2 \cdot k_{bf} + 2 \cdot \left(k_{np} - k_{bf}\right) \cdot \left(1+\beta\right)^3 \cdot \phi}{k_{np} + 2 \cdot k_{bf} - \left(k_{np} - k_{bf}\right) \cdot \left(1+\beta\right)^3 \cdot \phi} \tag{3}$$

The ratio of the nanolayer thickness to the original particle radius is represented by the parameter β in Eq. (3), and it is suggested to be equal to 0.1 (Duangthongsuk & Wongwises, 2010).

$$\mu_{nf} = \frac{\mu_{bf}}{\left(1-\phi\right)^{2.5}} \tag{4}$$

In order to define the heat transfer coefficient of the nanofluids, the Nusselt number is calculated. Because of that, the dimensionless numbers of Reynolds and Prandl need to be determined. Equations (5) and (6) present them respectively.

$$\mathrm{Re} = \frac{\rho_{nf} \cdot U_{nf} \cdot (2 \cdot r_{ai})}{\mu_{nf}} \tag{5}$$

$$\mathrm{Pr} = \frac{\mu_{nf} \cdot Cp_{nf}}{k_{nf}} \tag{6}$$

The nanofluid flows through the absorber tube of the PTC in a mass flow rate of 15 kg/s (m_{nf}). Thus, the flow velocity (U_{nf}) is then calculated with the Eq. (7) and the absorber tube area is determined with Eq. (8).

$$\dot{m}_{nf} = \rho_{nf} \cdot U_{nf} \cdot A_{ai} \tag{7}$$

$$A_{ai} = \pi \cdot r_{ai}^{\,2} \tag{8}$$

By the fact that this work studies different nanofluids, the Nusselt number is determined using different correlation, depending on nanoparticle material. For the case of pure Syltherm 800, the Dittus-Boelter correlation for turbulent flow is used (Adrian Bejan, 2004). Presented in Eq. (9), this correlation is valid for Reynolds number over 10,000 and Prandl number between 0.7 and 160.

$$Nu = 0.023 \cdot \mathrm{Re}^{0.8} \cdot \mathrm{Pr}^{0.4} \tag{9}$$

For the nanofluid composed with Al_2O_3 nanoparticles, Pak and Cho suggest the Eq. (10). This correlation is valid for Reynolds between 10,000 and 100,000 (Pak & Cho, 2013).

$$Nu = 0.021 \cdot \mathrm{Re}^{0.8} \cdot \mathrm{Pr}^{0.5} \tag{10}$$

For the case of TiO_2 nanoparticles it is used the Eq. (11), valid for Reynolds number between 3,000 and 28,000 (Duangthongsuk & Wongwises, 2010).

$$Nu = 0.074 \cdot \mathrm{Re}^{0.707} \cdot \mathrm{Pr}^{0.385} \cdot \left(100 \cdot \phi\right)^{0.074} \tag{11}$$

Finally, after determined Nusselt number, the nanofluid heat transfer coefficient (h_{nf}) is calculated with the Eq. (12) (Adrian Bejan, 2004).

$$h_{nf} = \frac{Nu \cdot k_{nf}}{(2 \cdot r_{ai})} \tag{12}$$

2.2 Solar collector field model

The solar field is based in a Parabolic Trough Collector (PTC), which consists in a long parabolic reflecting mirror pointed directly to the sun, and since the solar radiation is parallel, the light waves are reflected in a focal line. The three main parts of the PTC are: parabolic reflectors, receiver tube and the support structure (Olia et al., 2019). Figure 1 presents a schematic image of the PTC used in this work.

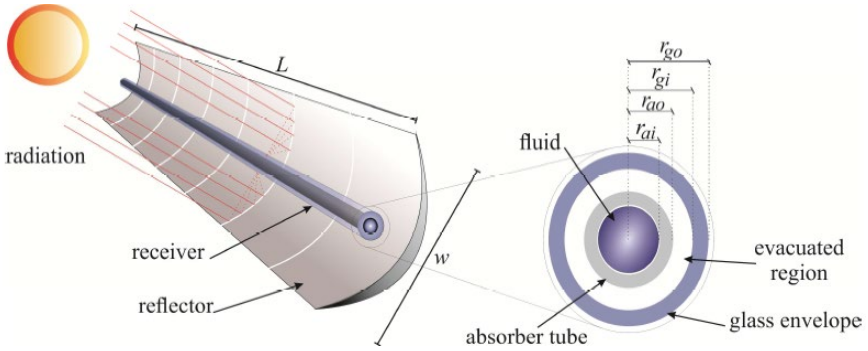

Figure 1. Schematic parabolic trough collector system.
Available from: (García et al., 2019)

The receiver tube is designed with two concentric tubes, the inner one made of copper, is defined as absorber tube, and the outer one made of glass, is defined as glass envelope. The nanofluid flows through the absorber tube and carries the heat acquired from the reflected radiation of the mirror. The Tab. 2 presents basic solar field parameters, PTC dimensions and materials constants.

Table 2. System constants parameters

Parameters	Value
Absorber inner radius (r_{ai})	0.033 m
Absorber outer radius (r_{ao})	0.035 m
Glass inner radius (r_{gi})	0.060 m
Glass outer radius (r_{go})	0.0625 m
Aperture width (w)	6 m
Aperture length (L)	12 m
Absorber emissivity (ε_a)	0.052
Glass emissivity (ε_g)	0.86
Optical efficiency (η_{opt})	0.741
Solar beam irradiation (Gb)	800 W/m²
Ambient temperature (Tamb)	25ºC
Stefan-Boltzmann constant (σ)	5.67E-8 W/m²K⁴

Parabolic Trough Collectors exploit the incident solar irradiation by reflecting it to the absorber tube. Thus, the PTC available solar energy (Q_s) is calculated as the product of the outer aperture area (A_{ap}), the solar beam irradiation (Gb) and the optical efficiency (η_{opt}) (Bellos & Tzivanidis, 2017).

$$Q_s = A_{ap} \cdot Gb \cdot \eta_{opt} \tag{13}$$

In order to define the PTC useful energy (Q_u), the present work takes into consideration the subtraction of the thermal losses (Q_{loss}) from the available solar energy (Q_s), as shows the Eq. (14).

$$Q_u = Q_s - Q_{loss} \tag{14}$$

The PTC thermal losses (Q_{loss}) are described by the sum of the absorber tube thermal losses ($Q_{a,loss}$), presented in Eq. (15) and the glass envelope thermal losses ($Q_{g,loss}$), presented in Eq. (16). It is important to state that the absorber tube thermal losses are only by radiation, the convection losses are neglected due to the vacuum between the absorber and the glass. Glass envelope thermal losses are by radiation and convection (Bellos et al., 2016; Qiu et al., 2017).

$$Q_{a,loss} = \frac{A_{a,os} \cdot \sigma \cdot (T_{ao}{}^4 - T_g{}^4)}{\frac{1}{\varepsilon_a} + \left(\frac{1-\varepsilon_g}{\varepsilon_g}\right) \cdot \frac{A_{a,os}}{A_{g,os}}} \tag{15}$$

$$Q_{g,loss} = A_{g,os} \cdot h_{out} \cdot (T_g - T_{amb}) + A_{g,os} \cdot \sigma \cdot \varepsilon_g \cdot (T_g{}^4 - T_{sky}{}^4) \tag{16}$$

The parameters T_g and T_{ao} represents the glass envelope temperature, assumed in this work as constant, and the absorber tube outer surface temperature, respectively. $A_{a,os}$ represents for the absorber outer surface area and $A_{g,os}$ for the glass outer surface area. The heat convection coefficient (h_{out}) is calculated with the Eq. (17). The wind velocity (U_{wind}) has a low impact on the results, due the evacuated tube, thus is selected as 1 m/s (Qiu et al., 2017).

$$h_{out} = 4 \cdot U_{wind}{}^{0.58} \cdot (2 \cdot r_{go})^{-0.42} \tag{17}$$

The sky temperature (T_{sky}) is estimated according to Eq. (18) (Evangelisti et al., 2019).

$$T_{sky} = 0.0553 \cdot T_{amb}{}^{1.5} \tag{18}$$

The glass envelope conduction is neglected, and the absorber tube walls (inner and outer) are assumed as isothermal in this work. The Eq. (19) describes the absorber tube wall heat transfer by conduction (Incropera et al., 2006).

$$Q_u = \frac{2 \cdot \pi \cdot L \cdot (T_{ai} - T_{ao}) \cdot k_a}{\ln\left(\frac{r_{ao}}{r_{ai}}\right)} \tag{19}$$

By defining the absorber tube inner wall temperature (T_{ai}) and the nanofluid heat transfer coefficient (h_{nf}), it is possible to calculate the PTC heat transfer rate, as the Eq. (20) presents (Adrian Bejan, 2004).

$$Q_{PTC} = \dot{m}_{nf} \cdot Cp_{nf} \cdot \Delta T_{in,col} \cdot \left[1 - \exp\left(-\frac{h_{nf} \cdot A_{a,is}}{\dot{m}_{nf} \cdot Cp_{nf}}\right)\right] \tag{20}$$

The variable $\Delta T_{in,col}$ represents the temperature difference between the absorber tube inner wall temperature and the nanofluid inlet temperature at the PTC. The parameter $A_{a,is}$ states for the absorber tube inner surface area and the Eq. (21) shows how it is determined.

$$A_{a,is} = 2 \cdot \pi \cdot r_{ai} \cdot L \tag{21}$$

2.3 ORC model

The Rankine cycle is the power cycle that is most often used in utility-scale electrical generation. It is an externally heated, steady flow system. The source of external heat is often provided by the combustion of coal or natural gas, but it can also be provided by nuclear, geothermal or solar energy (Klein & Nellis, 2011). The Organic Rankine Cycle (ORC) studied this work is externally heated by the energy carried from PTC through the nanofluid.

It is assumed in this work an ideal ORC in which the pump and turbine are considered isentropic and the friction losses in each of the four components are neglected. The four processes of the cycle are (Borgnakke & Sonntag, 2008):

1-2: Constant-pressure transfer of heat in the boiler;
2-3: Reversible adiabatic expansion;
3-4: Constant-pressure transfer of heat in the condenser;
4-1: Reversible adiabatic pumping process in the pump.

The present work selected the organic fluids Toluene and Cyclohexane as operation fluids of the ORC. It is important to state that these fluids properties are taken from the EES libraries.

Energy balances on the pump, boiler, turbine and condenser are presented in the following equations respectively (Klein & Nellis, 2011). This work considers the PTC heat transfer rate (Q_{PTC}) equal to the boiler heat transfer rate (Q_{boiler}). The parameter h states for the ORC working fluid enthalpy and the subscript for the cycle stage.

$$\frac{\dot{W}_{pump}}{\dot{m}_o} = h_1 - h_4 \tag{22}$$

$$\frac{\dot{Q}_{boiler}}{\dot{m}_o} = h_2 - h_1 \tag{23}$$

$$\frac{\dot{W}_{turb}}{\dot{m}_o} = h_2 - h_3 \tag{24}$$

$$\frac{\dot{Q}_{cond}}{\dot{m}_o} = h_3 - h_4 \tag{25}$$

The net power (W_{net}) and thermal efficiency (η_{ORC}) of the ORC are calculated according to the Eq. (26) and Eq. (27) respectively (Klein & Nellis, 2011).

$$\dot{W}_{net} = \dot{W}_{turb} - \dot{W}_{pump} \tag{26}$$

$$\eta_{ORC} = \frac{\dot{W}_{net}}{\dot{Q}_{boiler}} \tag{27}$$

This work assumes the boiler pressure (at stages 1 and 2) equal to 4 MPa, the temperature leaving the condenser (at stage 4) equal to the ambient temperature and the organic fluid mass flow rate (m_o) equal to 2 kg/s (Liu et al., 2017).

3. RESULTS AND DISCUSSIONS

The main objective of this work is to present the influence of the nanoparticles concentration on the PTC heat transfer rate and, consequently, in the ORC thermal efficiency. The analysis is made assuming the nanofluid inlet temperature in the PTC equal to 300ºC and taking into consideration the two different nanoparticles materials as well as the two different operation fluids of the ORC.

Figure 2 shows the behavior of the ORC thermal efficiency (η_{ORC}), when the nanoparticle concentration (ϕ) varies from 0.1 to 20%.

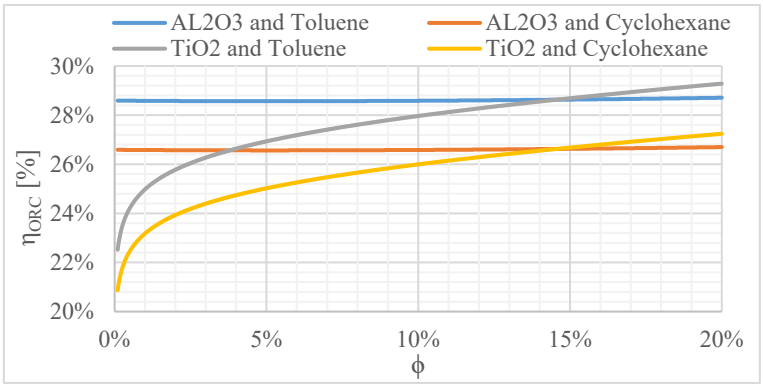

Figure 2. η_{ORC} variation with the increase of nanoparticles concentration

It is evident that, for both nanoparticle materials, the higher ORC performance is achieved using Toluene as operation fluid. It is also clear that the η_{ORC} behavior is very similar for each nanoparticle type, even working with different ORC operation fluid. It is important to state that the Al_2O_3 nanoparticles cause a slight influence in the cycle thermal efficiency, presenting its biggest η_{ORC} variation of 0.12%, from 28.59 to 28.71% for the cycle operating with Toluene. On the other hand, the TiO_2 nanoparticles show a significant enhancement in the cycle performance, from 22.52 to 29.28% for the cycle with Toluene.

PTC heat transfer rate is directly affected by the capacity of its working fluid to transport the heat absorbed from the sun. Figure 3 shows the behavior of the nanofluid heat transfer coefficient (h_{nf}) by varying its nanoparticle concentration (ϕ) from 0.1% to 20%. In addition, a comparison is made with the fluid without nanoparticle (pure Syltherm 800).

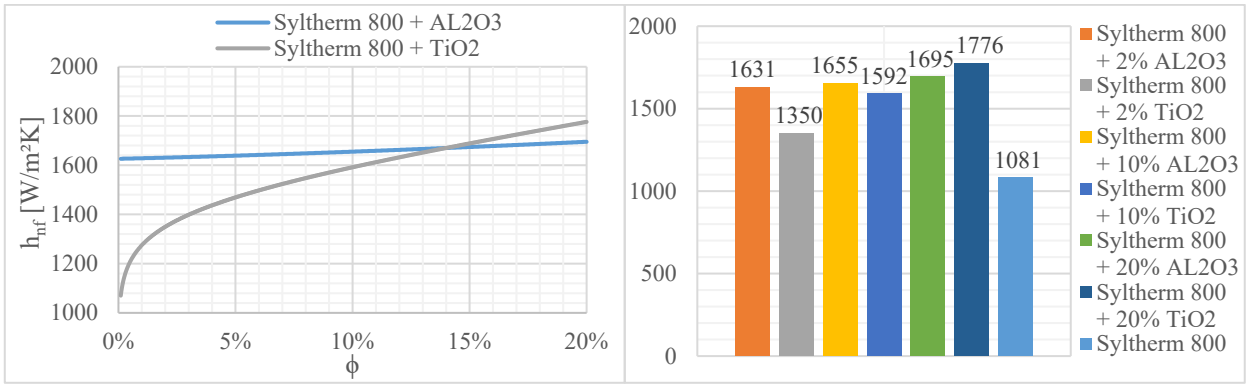

Figure 3. Nanofluid heat transfer coefficient variation with the increase of nanoparticles concentration

With low nanoparticle concentration, the nanofluid composed of Syltherm 800 and Al_2O_3 presents higher heat transfer coefficient, but the one composed of Syltherm 800 and TiO_2 shows a better improvement while the nanoparticle concentration increases, and after 14% of ϕ, a greater h_{nf} value than the other composition is demonstrated. It is also possible to observe that even with 2% of concentration, the nanofluids presents higher h_{nf} number when compared with pure Syltherm 800. At 2% of ϕ, the h_{nf} is already 550 and 269 W/m²K greater than pure Syltherm 800, for Al_2O_3 and TiO_2 nanoparticle, respectively. At 20% of ϕ, the nanofluids with Al_2O_3 and TiO_2 nanoparticles achieve 1695 and 1776 W/m²K, respectively, while the Syltherm 800, only 1081 W/m²K.

The increase of the nanoparticles concentration also provide a considerable change in Reynolds number. Taking from example the nanofluid composition of Syltherm 800 and TiO_2 nanoparticles, Figure 4 register the Reynolds variation while the TiO_2 concentration varies from 0.1 to 20%.

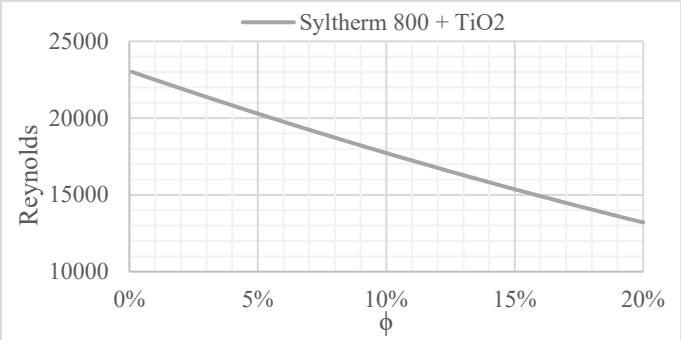

Figure 4. Reynolds variation with the increase of nanoparticles concentration

Figure 4 displays a huge drop of Reynolds number, from 23010, when nanoparticle concentration is 0.1%, to 13205, when it is 20%. By the fact that the Reynolds number is the ratio of inertial and viscosity forces of the fluid, it is possible to conclude that as the nanoparticles concentration increases, the nanofluid viscosity also increases. It is essential to state that this aspect is also noticed for the nanofluid composed of Syltherm 800 and Al_2O_3.

4. CONCLUSION

This work focused in the utilization of nanofluids, as the PTC working fluid, in order to upgrade this technology performance. The nanofluids were composed of Syltherm 800, as base fluid, and two different nanoparticle materials were evaluated, Alumina (Al_2O_3) and Titanium oxide (TiO_2). In addition, Toluene and Cyclohexane were investigated as operation fluids for the ORC. The PTC performance and, consequently, in the ORC thermal efficiency was studied by varying the nanoparticle concentration from 0.1 to 20%.

The nanofluid composed of Syltherm 800 and Al_2O_3 presented a small enhancement in the ORC thermal efficiency, from 28.59 to 28.71% when the cycle operated with Toluene. The nanofluid composed of Syltherm 800 and TiO_2 presented a considerable improvement, the ORC thermal efficiency increased 6.76%, from 22.52 to 29.28%, also operating with Toluene. The results for the ORC working with Cyclohexane showed similar behavior but lower numbers, for the nanoparticle concentration varying from 0.1 to 20%.

A comparison between the heat transfer coefficient of the nanofluids and pure Syltherm 800 was realized. The nanoparticle concentration also varied from 0.1 to 20% and the results demonstrated that the nanofluid composed of Syltherm 800 and Al_2O_3 displayed a slight heat transfer coefficient upgrade, from 1626 to 1695 W/m²K, the nanofluid composed of Syltherm 800 and TiO_2 showed a significant enhancement, from 1070 to 1776 W/m²K. The pure Syltherm 800 presented a heat transfer coefficient of 1081 W/m²K, which, at 2% of nanoparticle concentration, was already 550 and 269 W/m²K lower than the nanofluid composed with Al_2O_3 and TiO_2 nanoparticles, respectively.

The effect of nanoparticles concentrations in the Reynolds number was also analyzed. It is correct to affirm that higher concentrations denote greater viscosity forces, since the Reynolds number dropped from 23010 to 13205 while the concentration varied from 0.1 to 20%, for the nanofluid composed of Syltherm 800 and TiO_2.

In this way, it is possible to conclude that by the use of a specific composition and the appropriate amount of nanoparticles, a good enhancement can be found in the thermal efficiency of an ORC driven by PTC with the application of nanofluids.

5. ACKNOWLEDGEMENTS

The authors thank Pontifícia Universidade Católica de Minas Gerais (PUC Minas), the Conselho Nacional de Desenvolvimento Científico e Tecnologico (CNPq) “National Counsel of technological and scientific Development” and the Fundação de Amparo a Pesquisa de Minas Gerais (FAPEMIG) “Foundation for Research Support of Minas Gerais”. This study was financed in part by the Coordenação de Aperfeiçoamento de Pessoal de Nível Superior - Brasil (CAPES) - Finance Code 001.

6. REFERENCES

Abengoa. (2014). *Mojave Solar*. http://www.abengoa.com/web/en/index3.html

Abu-Hamdeh, N. H., & Almitani, K. H. (2016). Solar liquid desiccant regeneration and nanofluids in evaporative cooling for greenhouse food production in Saudi Arabia. *Solar Energy*, *134*, 202–210. https://doi.org/10.1016/j.solener.2016.04.048

Adrian Bejan. (2004). *Convection Heat Transfer* (Third). John Wiley&Sons, Inc.

Ayatollahi, M., Nasiri, S., & Kasaeian, A. (2012). *Convection Heat Transfer Modeling of Ag Nanofluid Using Different*

Viscosity CONVECTION HEAT TRANSFER MODELING OF AG NANOFLUID USING DIFFERENT VISCOSITY THEORIES. *April*. https://doi.org/10.31436/iiumej.v13i1.149

Bellos, E., & Tzivanidis, C. (2017). Parametric analysis and optimization of an Organic Rankine Cycle with nanofluid based solar parabolic trough collectors. *Renewable Energy*, *114*, 1376–1393. https://doi.org/10.1016/j.renene.2017.06.055

Bellos, E., & Tzivanidis, C. (2019). A review of concentrating solar thermal collectors with and without nanofluids. *Journal of Thermal Analysis and Calorimetry*, *135*(1), 763–786. https://doi.org/10.1007/s10973-018-7183-1

Bellos, E., Tzivanidis, C., Antonopoulos, K. A., & Daniil, I. (2016). The use of gas working fluids in parabolic trough collectors – An energetic and exergetic analysis. *Applied Thermal Engineering*, *109*, 1–14. https://doi.org/10.1016/j.applthermaleng.2016.08.043

Binotti, M., Zhu, G., Gray, A., Manzolini, G., & Silva, P. (2013). Geometric analysis of three-dimensional effects of parabolic trough collectors. *Solar Energy*, *88*, 88–96. https://doi.org/10.1016/j.solener.2012.10.025

Borgnakke, C., & Sonntag, R. E. (2008). *Fundamentals of Thermodynamics* (J. W. & S. Inc. (ed.); 7th Ed.). Don Fowley.

Choi, S. U. S., & Eastman, J. A. (1995). Enhancing thermal conductivity of fluids with nanoparticles. *American Society of Mechanical Engineers, Fluids Engineering Division (Publication) FED*, *231*(January 1995), 99–105.

Delfani, S., Karami, M., & Akhavan-Behabadi, M. A. (2016). Performance characteristics of a residential-type direct absorption solar collector using MWCNT nanofluid. *Renewable Energy*, *87*, 754–764. https://doi.org/10.1016/j.renene.2015.11.004

Dow Corning Corporation. (1997). *Syltherm 800 Heat Transfer Fluid*. https://www.dow.com/en-us/document-viewer.html?ramdomVar=7509246986654638378&docPath=/content/dam/dcc/documents/en-us/app-tech-guide/176/176-01435-01-syltherm-800-heat-transfer-fluid.pdf

Duangthongsuk, W., & Wongwises, S. (2010). An experimental study on the heat transfer performance and pressure drop of TiO 2 -water nanofluids flowing under a turbulent flow regime. *International Journal of Heat and Mass Transfer*, *53*(1–3), 334–344. https://doi.org/10.1016/j.ijheatmasstransfer.2009.09.024

Dupeyrat, P., Ménézo, C., & Fortuin, S. (2014). Study of the thermal and electrical performances of PVT solar hot water system. *Energy and Buildings*, *68*(PART C), 751–755. https://doi.org/10.1016/j.enbuild.2012.09.032

Evangelisti, L., Guattari, C., & Asdrubali, F. (2019). On the sky temperature models and their influence on buildings energy performance: A critical review. *Energy and Buildings*, *183*, 607–625. https://doi.org/10.1016/j.enbuild.2018.11.037

García, S. Q., Mora, H. S., Labarrios, M. A. P., & Ramírez, I. C. (2019). Modeling and simulation to determine the thermal efficiency of a parabolic solar trough collector system. *Case Studies in Thermal Engineering*, 100523. https://doi.org/10.1016/j.csite.2019.100523

Gorji, T. B., & Ranjbar, A. A. (2017). Thermal and exergy optimization of a nanofluid-based direct absorption solar collector. *Renewable Energy*, *106*, 274–287. https://doi.org/10.1016/j.renene.2017.01.031

Grena, R. (2010). Optical simulation of a parabolic solar trough collector. *International Journal of Sustainable Energy*, *29*(1), 19–36. https://doi.org/10.1080/14786450903302808

Incropera, F. P., DeWitt, D. P., Bergman, T. L., & Lavine, A. S. (2006). *Fundamentals of Heat and Mass Transfer* (John Wiley & Sons Inc. (ed.); 6th Ed.). Don Fowley.

Jaisankar, S., Ananth, J., Thulasi, S., Jayasuthakar, S. T., & Sheeba, K. N. (2011). A comprehensive review on solar water heaters. *Renewable and Sustainable Energy Reviews*, *15*(6), 3045–3050. https://doi.org/10.1016/j.rser.2011.03.009

Kalogirou, S. A. (2004). Solar thermal collectors and applications. In *Progress in Energy and Combustion Science* (Vol. 30, Issue 3). https://doi.org/10.1016/j.pecs.2004.02.001

Kalogirou, S. A., Karellas, S., Braimakis, K., Stanciu, C., & Badescu, V. (2016). Exergy analysis of solar thermal collectors and processes. *Progress in Energy and Combustion Science*, *56*, 106–137. https://doi.org/10.1016/j.pecs.2016.05.002

Khanafer, K., & Vafai, K. (2011). International Journal of Heat and Mass Transfer A critical synthesis of thermophysical characteristics of nanofluids. *International Journal of Heat and Mass Transfer*, *54*(19–20), 4410–4428. https://doi.org/10.1016/j.ijheatmasstransfer.2011.04.048

Klein, S., & Nellis, G. (2011). *Thermodynamics* (Cambridge University Press (ed.); First). www.cambridge.org/9780521195706

Lewis, N. S., & Nocera, D. G. (2007). Powering the planet: Chemical challenges in solar energy utilization (Proceedings of the National Academy of Science of the United States of America (2006) 103, 43, (15729-15735) DOI:10.1073/pnas.0603395103). *Proceedings of the National Academy of Sciences of the United States of America*, *104*(50), 20142. https://doi.org/10.1073/pnas.0710559104

Liu, P., Shu, G., Tian, H., Wang, X., & Jing, D. (2017). *Fluid Selection and Thermodynamic Analysis of anElectricity-Cooling Cogeneration System Based on Waste Heat Recovery fromMarine Engine (2) Fluid Selection and Thermodynamic Analysis of an Electricity-Cooling Cogeneration System Based on Waste Heat Recovery from Marine Engine*. *2011*. https://doi.org/10.4271/2017-01-0159

Maheshwary, P. B., Handa, C. C., & Nemade, K. R. (2017). A comprehensive study of effect of concentration, particle size and particle shape on thermal conductivity of titania/water based nanofluid. *Applied Thermal Engineering*, *119*, 79–88. https://doi.org/10.1016/j.applthermaleng.2017.03.054

Mahian, O., Kianifar, A., Sahin, A. Z., & Wongwises, S. (2014). International Journal of Heat and Mass Transfer Entropy generation during Al 2 O 3 / water nanofluid flow in a solar collector : Effects of tube roughness , nanoparticle size , and different thermophysical models. *HEAT AND MASS TRANSFER*, *78*, 64–75. https://doi.org/10.1016/j.ijheatmasstransfer.2014.06.051

Moran, M. J., Shapiro, H. N., Boettner, D. D., & Bailey, M. B. (2010). *Fundamentals of Engineering Thermodynamics* (J. W. & S. Inc. (ed.); 7th Ed.). Don Fowley.

Mwesigye, A., Huan, Z., & Meyer, J. P. (2015). Thermodynamic optimisation of the performance of a parabolic trough receiver using synthetic oil-Al2O3 nanofluid. *Applied Energy*, *156*, 398–412. https://doi.org/10.1016/j.apenergy.2015.07.035

Nagarajan, P. K., Subramani, J., Suyambazhahan, S., & Sathyamurthy, R. (2014). Nanofluids for solar collector applications: A review. *Energy Procedia*, *61*(January), 2416–2434. https://doi.org/10.1016/j.egypro.2014.12.017

Olia, H., Torabi, M., Bahiraei, M., Ahmadi, M. H., Goodarzi, M., & Safaei, M. R. (2019). Application of nanofluids in thermal performance enhancement of parabolic trough solar collector: State-of-the-art. *Applied Sciences (Switzerland)*, *9*(3). https://doi.org/10.3390/app9030463

Owusu, P. A., & Asumadu-Sarkodie, S. (2016). A review of renewable energy sources, sustainability issues and climate change mitigation. *Cogent Engineering*, *3*(1), 1–14. https://doi.org/10.1080/23311916.2016.1167990

Pak, B. C., & Cho, Y. I. (2013). Hydronamic and heat transfer study of dispersed fluids with submicron metallic oxide. *Experimental Heat Transfer: A Journal of Thermal Energy Generation, Transport, Storage, and Conversion*, *January 2013*, 37–41.

Qiu, Y., Li, M. J., He, Y. L., & Tao, W. Q. (2017). Thermal performance analysis of a parabolic trough solar collector using supercritical CO2 as heat transfer fluid under non-uniform solar flux. *Applied Thermal Engineering*, *115*, 1255–1265. https://doi.org/10.1016/j.applthermaleng.2016.09.044

Turkyilmazoglu, M. (2017). Condensation of laminar film over curved vertical walls using single and two-phase nanofluid models. *European Journal of Mechanics B/Fluids*. https://doi.org/10.1016/j.euromechflu.2017.04.007

Tzivanidis, C., Bellos, E., & Antonopoulos, K. A. (2016). Energetic and financial investigation of a stand-alone solar-thermal Organic Rankine Cycle power plant. *Energy Conversion and Management*, *126*, 421–433. https://doi.org/10.1016/j.enconman.2016.08.033

U.S. Energy Information Administration. (2019). *EIA projects nearly 50% increase in world energy usage by 2050, led by growth in Asia*. https://www.eia.gov/todayinenergy/detail.php?id=41433#

United Nations. (2019). *WPP2019_POP_F01_1_TOTAL_POPULATION_BOTH_SEXES*. http://creativecommons.org/licenses/by/3.0/igo/

Xu, G., Fu, J., Dong, B., Quan, Y., & Song, G. (2019). A novel method to measure thermal conductivity of nanofluids. *International Journal of Heat and Mass Transfer*, *130*, 978–988. https://doi.org/10.1016/j.ijheatmasstransfer.2018.11.014

Yu, W., & Choi, S. U. S. (2003). *The role of interfacial layers in the enhanced thermal conductivity of nanofluids : A renovated Maxwell model*. 167–171.

Zamzamian, A., KeyanpourRad, M., KianiNeyestani, M., & Jamal-Abad, M. T. (2014). An experimental study on the effect of Cu-synthesized/EG nanofluid on the efficiency of flat-plate solar collectors. *Renewable Energy*, *71*, 658–664. https://doi.org/10.1016/j.renene.2014.06.003

Zhang, L., Chen, L., Liu, J., Fang, X., & Zhang, Z. (2016). Effect of morphology of carbon nanomaterials on thermo-physical characteristics, optical properties and photo-thermal conversion performance of nanofluids. *Renewable Energy*, *99*, 888–897. https://doi.org/10.1016/j.renene.2016.07.073

7. RESPONSIBILITY NOTICE

The authors are the only responsible for the printed material included in this paper.